The Negishi Catalysis: Full Study of the Complications in the Transmetalation Step and Consequences for the Coupling Products

Juan del Pozo,[1] Gorka Salas,[2] Rosana Álvarez,*[3] Juan A. Casares,*[1] and Pablo Espinet*[1]

[1] IU CINQUIMA/Química Inorgánica, Facultad de Ciencias, Universidad de Valladolid, 47011-Valladolid (Spain)

[2] IMDEA Nanociencia, Ciudad Universitaria de Cantoblanco, 28049 Madrid, Spain.

[3] Departamento de Química Orgánica, Facultad de Química (CINBIO), Universidade de Vigo. Campus As Lagoas-Marcosende, 36310 Vigo (Spain)

ABSTRACT: In addition to the expected products, *trans*- and *cis*-[PdRfMe(PPh$_3$)$_2$], the transmetalation between ZnMe$_2$ and *trans*-[PdRfCl(PPh$_3$)$_2$] yields [PdMeCl(PPh$_3$)$_2$] and ZnRfMe as the result of secondary transmetalation processes. ZnRfMe is also formed by reaction of *trans* and *cis*-[PdRfMe(PPh$_3$)$_2$] with ZnMe$_2$. The different competitive reaction mechanisms that participate in the transmetalations have been studied experimentally and by DFT calculations. The relative contribution of each reaction pathway in the formation of the unwanted product ZnRfMe has been measured. The effect of excess ligand (PPh$_3$) on the several transmetalations has been stablished.

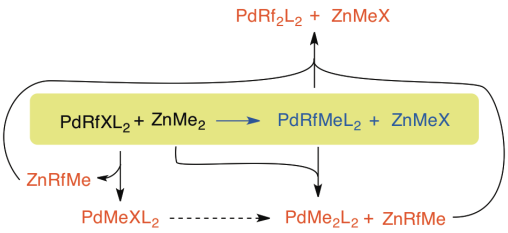

INTRODUCTION

The Negishi reaction is a powerful process for the formation of C-C bonds.[1,2] In fact, it is the reaction of choice for couplings involving sp^3 carbons, due to the high reactivity of organozinc reagents.[3,4,5] The coupling of alkylgroups from organoboron and organotin organometallics is usually very sluggish unless highly nucleophilic activators are used to facilitate the transmetalation step. In sharp contrast, organozincs have been shown to transmetalate to Pd at temperatures as low as −60 °C,[6] which allows for remarkably facile coupling of alkyl groups, even secondary ones.[7] As for other palladium catalyzed couplings of organic electrophiles (R^{1}X) and nucleophiles (MR^2), the reaction pursues the selective formation of R^1–R^2, but frequently homocoupling byproducts, presumably formed via undesired transmetalations, contaminate the result.[8] In 1994 van Asselt and Elsevier showed that these homo-coupling products could arise from undesired reactions that exchange the organic group in the nucleophile by another organic group at the palladium, rather than by the halogen (Scheme 1a). Thus, in the reaction of [PdBzBr(ArBIAN)] (Bz = benzyl; Ar-BIAN = bis(arylimino)acenaphthene) with ZnTolCl they found that the exchange produced the observable Bz/Tol intermediate [PdTolBr(ArBIAN)], which after subsequent Br/Tol transmetalation led to (MeC$_6$H$_4$)$_2$ as the main reaction product.[9]

A second report, this time involving C(sp^3) in the coupling, came some years later from our group, when we found that the transmetalation of *trans*-[PdRfCl(PPh$_3$)$_2$] (**1**) (Rf = 3,5-dichloro-2,4,6-trifluorophenyl) with ZnMe$_2$ or with ZnMeCl produced, in addition to the two expected palladium complexes *trans*-[PdRfMe(PPh$_3$)$_2$] (**2**) and *cis*-[PdRfMe(PPh$_3$)$_2$] (**3**), large amounts of ZnRfMe, ZnRfCl, and [PdMe$_2$(PPh$_3$)$_2$].[10] Following our observation Lei *et al.* reported the formation of undesired aryl exchanges between zinc and palladium (Scheme 1b), as well as the formation of homocoupling biaryls, in the Pd catalyzed coupling of Ar^{1}I with ZnAr^{2}Cl.[11a] They suggested that the Ar^1-Ar^2 to Ar^2-Ar^2 ratio found in the products was the result of the kinetic competition between reductive elimination and aryl exchange reaction rates on a [PdAr^{1}Ar^2(dppf)] intermediate.

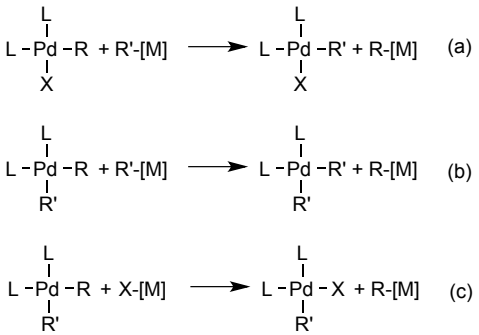

Scheme 1. Previous results

In Negishi syntheses, where halides are always present (introduced in the initial oxidative addition step of ArX to Pd^0), the study of the undesired reactions shown in Scheme 1 (equations a and b) is obscured by the interference of re-

trotransmetalation reactions (Scheme 1c).[12,] A good starting point to analyze these complicated system is to dissect the study starting on the reactivity of complexes [PdArAr'L_2] with ZnR_2 derivatives, which provides a particular scenario where halides (hence reactions a and b in Scheme 1) are absent. These complexes are well known intermediates in cross-coupling reactions. The reductive elimination of two sp^2 carbons from *cis*-[PdArAr'L_2] is usually fast,[13] but in instances that disfavor reductive elimination (e.g. electron withdrawing groups in the carbon fragments, or large steric hindrance), the undesired transmetalations shown in Scheme 1a-c can become a serious competition to the expected Ar–Ar' cross-coupling.[14] Furthermore, the reductive elimination step in coupling reactions involving sp^3 carbon atoms is usually slow,[13] and when seeking for Ar–alkyl couplings reactions these undesired transmetalations may become an efficient via to undesired Ar-Ar products.[8] Moreover, we have recently shown that there are cis/trans isomerization reactions of [PdRR'L_2] complexes (R = Me; R' = Me or 3,5-dichloro-2,4,6-trifluorophenyl (Rf)) that are mechanistically associated to transmetalations because they share a common intermediate. This further complicates the reaction scheme during the cross-coupling reaction.[15] From a positive point of view, all these model systems with high coupling barriers to the desired product create a landscape where the undesired side processes can be more easily studied.

Herein we report kinetic experiments and DFT computational studies to understand the complications disturbing the desired ideal Negishi process, by examining the reactivity of [PdMeArL_2] (*cis* and *trans*, Ar = C_6F_5, $C_6F_3Cl_2$) complexes with $ZnMe_2$ and other secondary transmetalations. The computational studies provide features of the structures participating in the transmetalations, stereochemistry at palladium, additional intermediates or transition states that cannot be kinetically deduced, structural details of the exchange process, etc.[16] The graphical presentation of the process is made in a unified manner, so the reaction profiles will contain experimental and calculated values for comparison but, obviously, not every calculated structure has a measured experimental energy. For instance, energies of species after the rate determining state cannot be experimentally measured.[17]

Results and discussion

In the Negishi process (also in others) we can define two categories of transmetalation, depending on the groups undergoing exchange: *i)* primary transmetalations, in which an R group on Zn is exchanged for an X group (usually a halide) on Pd (*X for carbon exchange*); *ii)* secondary transmetalations, meaning transmetalations that exchange two R fragments between Pd and Zn (*carbon for carbon exchanges*). Other possible combinations as transmetalations where an X group on Zn were exchanged for an R group on Pd are usually thermodinamically unfavorable.

The first step in the PdL_n-catalyzed (L = PPh_3) Negishi coupling of RfX (X^- = halide) with $ZnMe_2$ is the oxidative addition of RfX to PdL_n, producing [PdRfXL_2] (**1**, Rf = $C_6F_3Cl_2$).[18] Then, in the transmetalation step, only the exchanges involving non-identical groups are synthetically relevant and observable by NMR, in addition to the isomerization of the Pd complexes. With these conditions, the most relevant exchanges of different groups (taken in both senses of the equilibrium) are shown in Chart 1.[19]

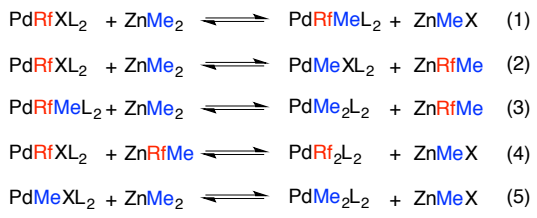

Chart 1. Primary and secondary transmetalations (cis/trans isomers not specified for simplicity).

The only desired transmetalation (X for Me) is the primary transmetalation in Eq. 1, leading to [PdRfMeL_2], which is the complex precursor of the cross-coupling product. However, an undesired secondary transmetalation (Rf for Me) can take place with the same reagents (Equation 2), leading to [PdMeXL_2]. Another possible undesired secondary transmetalation (Eq. 3) consumes [PdRfMeL_2] to produce undesired $PdMe_2L_2$, a potential source of Me–Me homocoupling. Equations 1, 2, and 3 produce previously inexistent Pd complexes or Zn reagents that are a potential source of new primary transmetalations, now undesired, as shown in Eq. 4 (forming a potential source of Rf–Rf homocoupling), and Eq. 5 (along with Eq. 3, forming a potential source of Me–Me homocoupling).

To organize the discussion we are considering the exchanges in three sections.

1.- Analysis of the primary Cl/Me transmetalation exchange on trans-[PdRfCl(PPh_3)$_2$] (1) with $ZnMe_2$, complicated by secondary Rf/Me transmetalations.

Some time ago we reported that the transmetalation reaction between *trans*-[PdRfCl(PPh_3)$_2$] (**1**) and $ZnMe_2$, run at 25°C in THF with a 20:1 excess of $ZnMe_2$, produces *trans* and *cis*-[PdRfMe(PPh_3)$_2$] (**2** and **3,** respectively) and ZnMeCl, but also a large amount of the exchange products ZnRfMe and [$PdMe_2$(PPh_3)$_2$] (Scheme 2).[10]

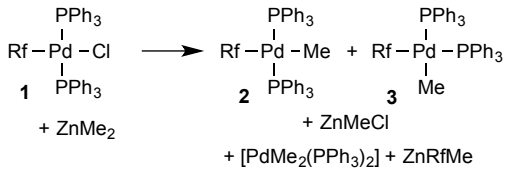

Scheme 2. Our previous results in reference 10.

We have studied here the effect of an excess of ligand in that system. Figure 1 plots the disappearance of **1**, and the formation of the different products, in the reaction of *trans*-[PdRfCl(PPh_3)$_2$] (**1**) with a fixed excess of $ZnMe_2$ (Zn:Pd = 10 : 1), in solutions with increasing amount of PPh_3.

The data in Figure 1 show that the rate of consumption of **1** depends on $[PPh_3]^{-1}$, meaning that, as in many other transmetalation processes with other nucleophiles, the first

step in the transmetalation involves the substitution of PPh_3 by the incoming $ZnMe_2$. The same holds for the initial formation of *trans*-[PdRfMe(PPh_3)$_2$] (**2**), which is the main product at short reaction times, and ZnClMe (non detectable in the ^{19}F spectrum).

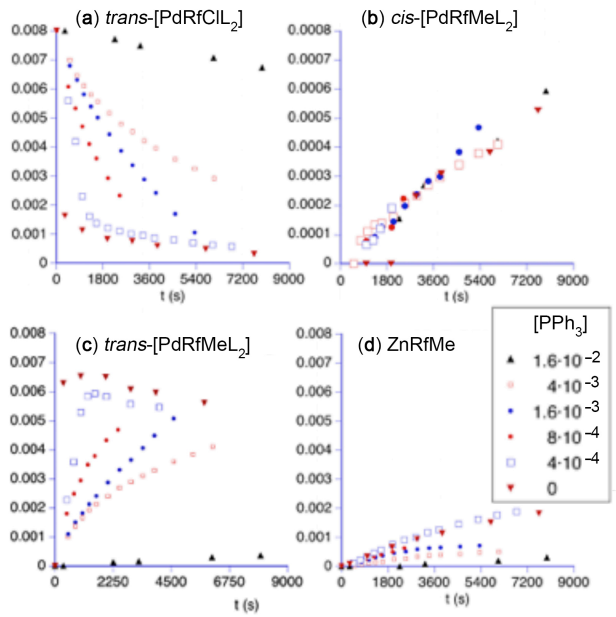

Figure 1. Experimental concentration versus time plots for the transmetalation reaction of *trans*-[PdRfCl(PPh_3)$_2$] with $ZnMe_2$ under different concentrations of PPh_3. Traces of (a) *trans*-[PdRfCl(PPh_3)$_2$] (**1**), (b) *cis*-[PdRfMe(PPh_3)$_2$] (**3**), (c) *trans*-[PdRfMe(PPh_3)$_2$] (**2**) and (d) ZnRfMe. Note the different scale for the concentrations of *cis*-[PdRfMeL$_2$] (Figure 1b). The data have been obtained by integration of ^{19}F NMR spectra.

Regarding the formation of *cis*-[PdRfMe(PPh_3)$_2$] (**3**) and ZnRfMe, interpretation of the data is less clear cut: their experimental kinetic orders are 0.2 and 0.3 respectively,[20] suggesting that these species are involved in several reactions that have different dependence on the concentration of PPh_3. We have shown in a previous study that the isomerization of **3** to **2** is phosphine dependent and can be catalyzed by $ZnMe_2$.[15] For ZnRfMe the situation is even more complex since ZnRfMe is formed by two ways: ***i***. through the secondary transmetalations between **2** or **3** and $ZnMe_2$; and ***ii***. by direct Me/Rf exchange between **1** and $ZnMe_2$. The dependence of these processes on the concentration of PPh_3 has not been established so far. There are other possible sources of ZnRfMe, such the retrotransmetalation of ZnMeCl with **2** or **3**, but these are not significant under the very low concentration of ZnMeCl existing at the beginning of the reaction, consequently retrotransmetalation pathways cannot explain the high rate of formation of ZnRfMe observed at short reaction times.

Although the bizarre kinetic order for the formation of cis-[PdRfMe(PPh_3)$_2$] (**3**) and ZnRfMe suggests the competition of several mechanisms, it is not possible to quantify the reaction parameters unless the reactions of **2** and **3** with $ZnMe_2$ are addressed first.

2.- Analysis of the secondaryRf/Me transmetalation exchanges on trans- and cis-[PdRfMe(PPh$_3$)$_2$] with ZnMe$_2$. The reactions of *trans*- and *cis*-[PdMeRf(PPh_3)$_2$] (**2** and **3**, respectively) with $ZnMe_2$ in THF were studied at 298° K monitoring the Rf/Me exchange by ^{19}F and ^{31}P NMR. When a large excess of $ZnMe_2$ was employed (as it is the conditions of Negishi cross-coupling reactions), the transmetalation equilibrium was shifted towards the formation of the ZnRfMe. Under these conditions the isomerization *trans* to *cis*-[PdMe$_2$(PPh_3)$_2$] is very fast, so eventually both isomers, *cis*- and *trans*-[PdRfMe(PPh_3)$_2$], are transformed into *cis*-[PdMe$_2$(PPh_3)$_2$], which is the thermodynamically highly favored isomer (Scheme 3).

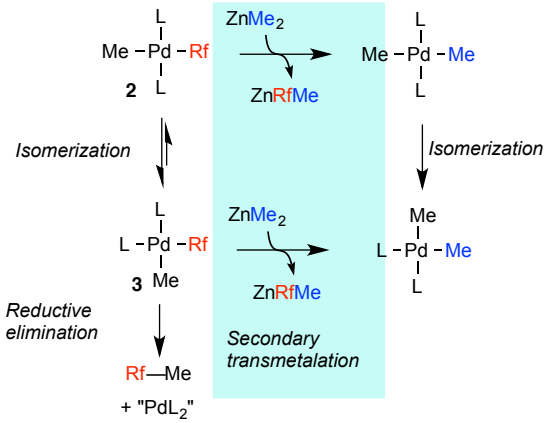

Scheme 3. Formation of *cis*-[PdMe$_2$L$_2$] by secondary transmetalations involving complexes **2** and **3**.

The reaction rates were been measured in experiments with added PPh_3.[21] In these conditions the kinetic influence of reductive elimination of Rf–Me or Rf–Rf is negligible. The reaction orders on the concentration of PPh_3 were obtained for **2** and **3** from the initial rates, and kinetic rate constants were obtained by non-linear-least-square fitting of the data. The experimental $\Delta G^{\ddagger}_{\ddagger}$ values are represented, along with the calculated ones, in the reaction profile in Figure 2.

The experimental studies for the *cis* isomer **3** show that the free ligand retards the formation of ZnRfMe. The process is roughly order minus one (slope –0.9 based on initial rates of formation of ZnRMe, see SI) with respect to the concentration of PPh_3, and the plot of r_0^{-1} versus the concentration of PPh_3 added is a straight line. This is consistent with a mechanism in which the first step is the substitution of one phosphine ligand by $ZnMe_2$, producing an intermediate [PdRfMeL–$ZnMe_2$], prior to the transmetalation step (equations 6–8 in Chart 2). Fitting the experimental values to this model, the activation energies for the phosphine dissociation (22.4 kcal/mol) and for the Rf/Me exchange (25.7 kcal/mol) were obtained for complex **3**.

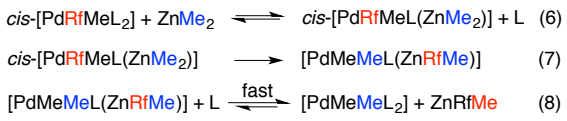

Chart 2. Proposed mechanism for Me/Rf exchange between Zn and Pd in the reaction of *cis*-[PdRfMe(PPh_3)$_2$] (**3**) with $ZnMe_2$.

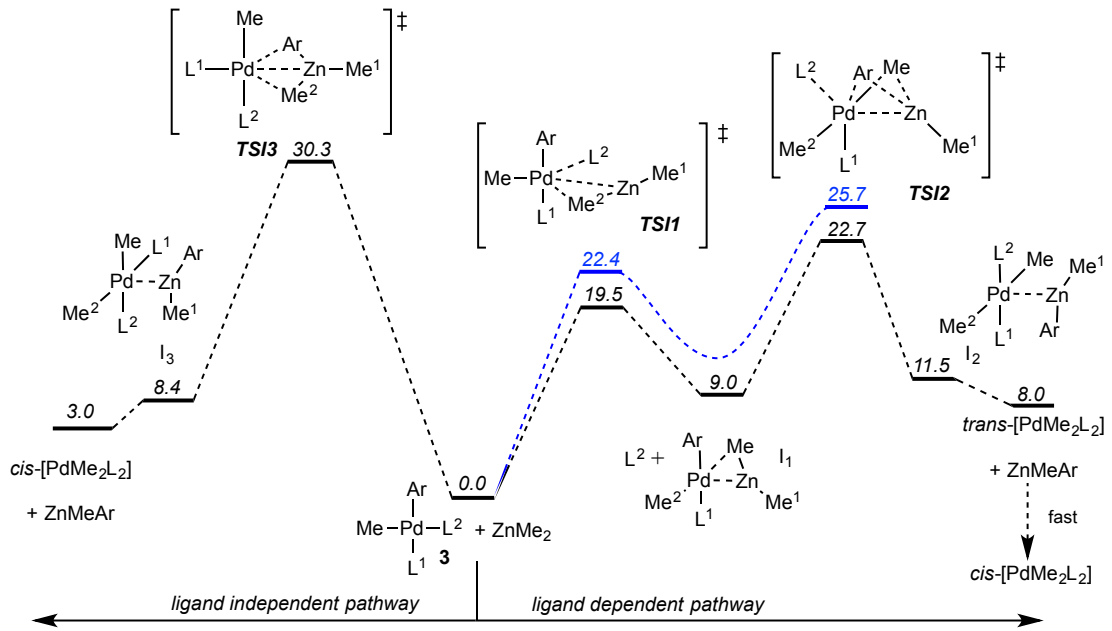

Figure 2. DFT profiles (wB97XD/PCM(THF)/6-31G*-SDD//B3LYP/6-31G*-SDD; Ar = Pf and $L_1 = L_2 = PPh_3$), and experimental energy values (blue, Ar = Rf) for the mechanisms proposed for the secondary transmetalation (ligand dependent and independent pathways) in the reaction between *cis*-[PdArMe(L)$_2$] **3** and $ZnMe_2$ ($\Delta G^{\pm}$ are given in kcal/mol). Obviously the calculated energy for the intermediate connecting ***TSI1*** and ***TSI2*** makes its formation slower than its disappearance, so it cannot be observes experimentally.

The proposed pathways were studied by DFT methods (wB97XD/PCM(THF)/6-31G*-SDD//B3LYP/6-31G*-SDD), and the results are shown in Figure 2.[22,23,24] The overall mechanism resembles a double substitution process and it is similar to that found for the $ZnMe_2$ catalyzed isomerization of **3** to **2**.[15]

Starting with *cis*-[PdArMe(L)$_2$] (**3**) and following the ligand substitution pathway in Figure 2, the calculations propose first a very weak interaction between $ZnMe_2$, which was commented on in a previous paper and has no kinetic significance.[15] In the transition state ***TSI1*** the Zn-Me^2 bond acts as incoming ligand releasing one PPh_3 (L^2) from the palladium, while the zinc takes electron density from the Rf–Pd bond, affording intermediate **I$_1$**, with the exchanging Me involved in a 3c-2e bond. The second substitution takes place so that the incoming ligand is PPh_3 and the leaving ligand is the Rf–Zn bond (***TSI2***). The activation energy for these transition states (19.5 and 22.7 kcal/mol, respectively) fit very well with the experimental values obtained (22.4 and 25.7 kcal/mol, respectively). Note that this pathway produces *cis* to *trans* isomerization of the PPh_3 ligands yielding *trans*-[PdMe$_2$L$_2$], but the $ZnMe_2$ catalyzed isomerization to *cis*-[PdMe$_2$L$_2$] is fast.

The putative reaction without ligand substitution for *cis*-[PdArMe(L)$_2$] was also studied by DFT (Figure 2, ligand-independent mechanism) and consists in a rather common associative exterchange of Me and Rf via a double-bridge (with Pd–Zn bond participation). The PPh_3 ligands remain *cis* throughout the process. The participation of this pathways looks unimportant since it shows a much higher activation energy (30.3 kcal/mol).

The reaction of *trans*-[PdRfMe(PPh$_3$)$_2$] with $ZnMe_2$ was studied under the same experimental conditions. In this case the dependence of the reaction rate on the concentration of PPh_3 was very small (the experimental order of the secondary transmetalation reaction is -0.3). This suggests the participation of two competitive pathways, one independent of the phosphine concentration and another (slower but not negligible) dependent (Scheme 4). The experimental data fit well to this kinetic model, although the system contains too many variables to be fully resolved.[25,26]

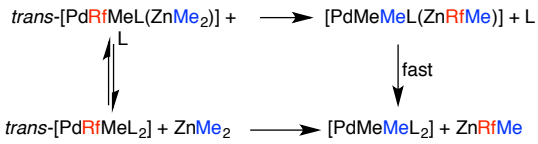

Scheme 4. Rf/Me secondary transmetalation on *trans*-[PdRfMe(PPh$_3$)$_2$].

Figure 3 shows the DFT profiles starting with *trans*-[PdArMe(L)$_2$] (**2**) and $ZnMe_2$ for both mechanisms (ligand substitution and no-ligand-dependent mechanisms). The ligand substitution pathway that takes place in one single step (ligand-independent), is again an associative exchange of Me and Rf via a double-bridged transition state ***TSI6.*** The calculated activation energy is $\Delta G^{\pm}$ = 26.4 kcal/mol (experimental, 23.7 kcal/mol). As for the *cis* complex, there is no PPh_3 isomerization in this pathway.

The higher efficiency of the direct Rf/Me exchange in the *trans* complex **2**, confirming lower activation energy than for the *cis* complex **3**, is due to the large *trans*-influence of the Me group, which induces electron density into the Ar group,

making the bridge where it participates in ***TSI6*** less electron deficient, consequently stabilizing this transition state. Although the product of transmetalation through this pathway is *trans*-[$PdMe_2L_2$], in the reaction conditions it isomerizes fast to *cis*-[$PdMe_2L_2$] as already discussed.

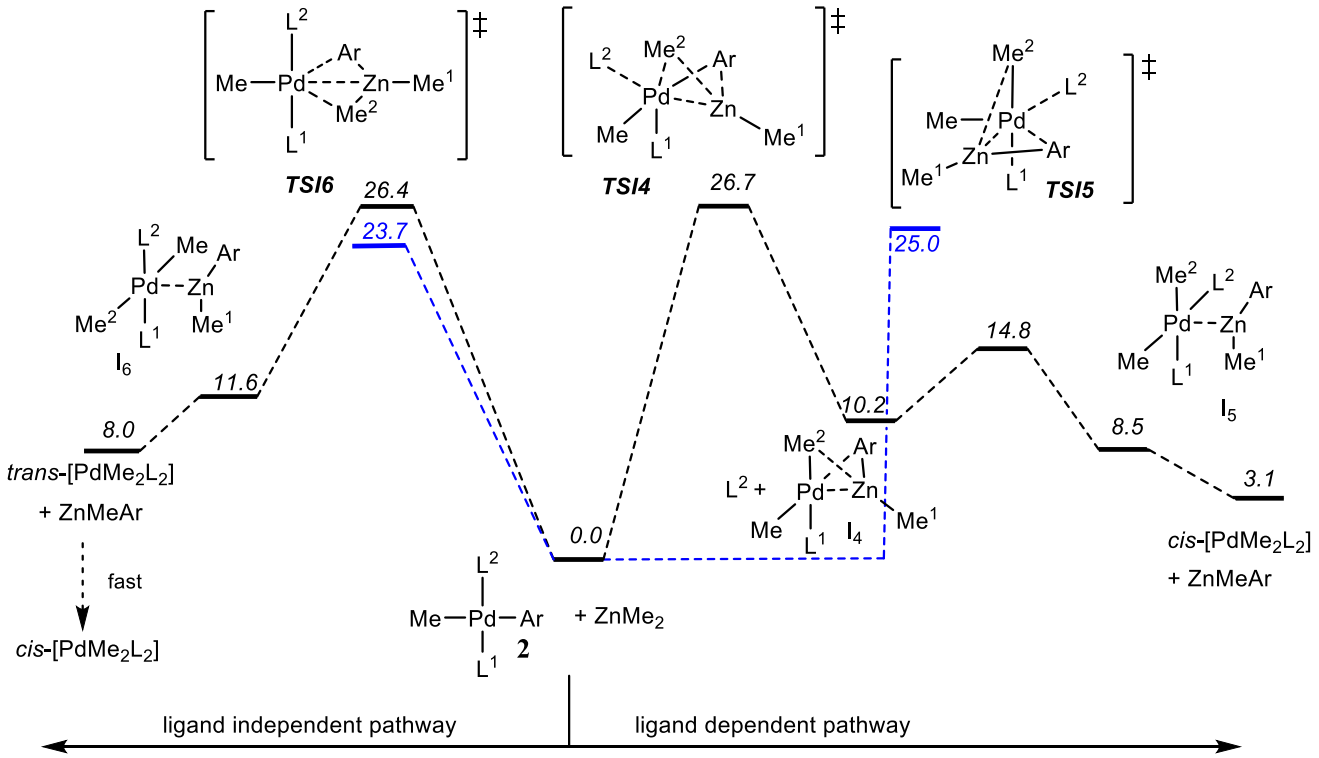

Figure 3. DFT profiles (wB97XD/PCM(THF)/6-31G*-SDD//B3LYP/6-31G*-SDD; green Ar = Pf and $L_1 = L_2 = PPh_3$), and experimental energetic values (blue, Ar = Rf) for the mechanisms proposed for the secondary transmetalation (ligand dependent and independent pathways) in the reaction between *trans*-[PdArMe$(L)_2$] **2** and $ZnMe_2$ ($\Delta G^{\pm}$ are given in kcal/mol).

The phosphine-dependent pathway starting from the *trans* isomer, (Figure 3) is a double substitution process similar to that discussed above for the reaction of the *cis* isomer, and for the previously reported isomerization catalyzed by $ZnMe_2$ of **2** to **3**.[15] It yields directly *cis*-[$PdMe_2L_2$]. The activation energy is very similar to the phosphine independent pathway and this explains the -0.3 dependence order on PPh_3 concentration.

The studies in this section show that both isomers, **2** and **3**, are able to suffer secondary transmetalations under the conditions in which the main reaction (primary transmetalation on **1**) takes place, eventually producing *cis*-[$PdMe_2L_2$]. With PPh_3 as ligand, the ligand-independent pathway prevails for **3**, and is in competition with the ligand-dependent pathways for **2**. Due to these ligand-independent pathways, the addition of excess of ligand cannot completely inhibit the secondary transmetalations. It looks that one plausible solution to suppress them might be the use of ligands that make stronger Pd-L bonds: that would inhibit their substitution by alkylzinc reagents, quenching the ligand dependent pathway. Calculations for the stronger ligand PMe_3 for comparison (Table 1) show a more complex behavior.[24] For complex **3** and the ligand-dependent pathway (Figure 2) the rate determining $\Delta G^{\pm}$ certainly increases from 22.7 to 23.9 kcal. mol^{-1}, but this difference involves a change of transition state from ***TSI2*** to ***TSI1***. In fact the large effect upon ligand change occurs in ***TSI1***, which changes from 19.5 to 23.9 kcal. mol^{-1}. Also a significant change is produced in the competitive ligand independent pathway, for which ***TSI3*** changes from 30.3 to 25.7 kcal/mol, increasing its global contribution to the reaction. However, for complex **2** and the ligand-dependent pathway transition (Figure 3) a small decrease in $\Delta G^{\pm}$ from 26.7 to 24.3 kcal.mol^{-1}, this time associated to only one transition state (***TSI4***) is observed, whereas the large increase (from 14.8 to 23.4 kcal.mol^{-1}) occurs in ***TSI5*** and is insufficient to produce an overall increase for this pathway. For this isomer the stabilization of ***TSI6*** (from 26.4 to 22.7 kcal/mol) in the ligand independent pathway makes of it the favorite for L = PMe_3, frustrating the otherwise beneficial effect of using a strong donor ligand. Thus, how much the transition states are affected is not easy to guess when comparing the *cis* and the *trans* isomers.

Table 1. $\Delta G^{\pm}$ (kcal/mol) for the transition states of the pathways in the reaction between *trans* or *cis*-[PdArMe$(L)_2$] (**2** or **3**) and $ZnMe_2$ (L = PMe_3 or PPh_3).

	3			**2**		
	TSI1	***TSI2***	***TSI3***	***TSI4***	***TSI5***	***TSI6***
PMe_3	23.9	21.4	25.7	24.3	23.4	22.7
PPh_3	19.5	22.7	30.3	26.7	14.8	26.4

Somehow against our initial expectations, the transition states of the simpler ligand-independent pathway are highly stabilized for the better donor ligand PMe_3 for both isomers (***TSI3*** and ***TSI6***) and the secondary transmetalations become more competitive, totally frustrating this solution to the problem. In fact, the transition state of the pathways that we have been calling "ligand-independent" because ligand is not released, are ligand dependent through the electronic effect of the ancillary ligand on the bridges, which are less electron deficient for stronger donor ancillary ligands.

From a practical point of view the conclusion of this section is that the best way to address this problem and reduce the incidence of these undesired secondary transmetalations seems to be the use ligands that accelerate the reductive elimination.

3.- Analysis of the secondary Rf/Me transmetalation exchange on trans-[PdRfCl(PPh$_3$)$_2$] 1 with ZnMe$_2$. Now, having determined independently the rates for the isomerization between **2** and **3**, and for the secondary Rf/Me transmetalations in the reaction between *cis*- or *trans*-[PdArMe(PPh_3)$_2$] and $ZnMe_2$, it is possible to revisit our initial study on *trans*-[PdRfCl(PPh_3)$_2$]. Figure 4 shows the course of the transmetalation experiment of *trans*-[PdRfCl(PPh_3)$_2$] **1** and $ZnMe_2$. In order to fit the observed results we carry out an overall kinetic simulation including the primary Cl/Me substitution and all the previous observations (Scheme 5), and taking into account the isomerization and the two profiles (ligand-dependent and no-ligand-independent mechanisms) discussed in the previous section. In these simulations the rate constants of the secondary transmetalations on **2** and **3**, the **2**/**3** isomerization, and the reductive elimination from **3** have been taken from experimental values reported in our previous works with the same system.[10,15]

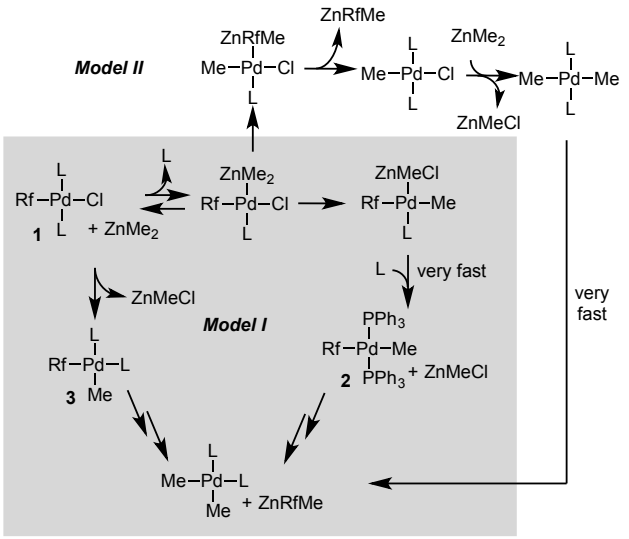

Scheme 5. The overall mechanism of the transformations in the reaction between [PdRfCl(PPh_3)$_2$] **1** and $ZnMe_2$.

Model I proposes the transmetalation of **1** with $ZnMe_2$ to afford 2 through a ligand-dependent pathway, thus including the formation of intermediates in which the ligand *cis*- to the chlorine has been displaced by $ZnMe_2$.[27] On the other hand a competitive ligand-independent transmetalation, produces **3**, in concordance with the experimental behavior of the system.[28] This model fits well the observed kinetic reaction order relative to the concentration of PPh_3, but not the formation of ZnRfMe (red solid spots in Figure 6a), as it predicts very low concentration of ZnRfMe until almost all the starting palladium complex has been transformed into **2** and **3**, which is not the case observed.

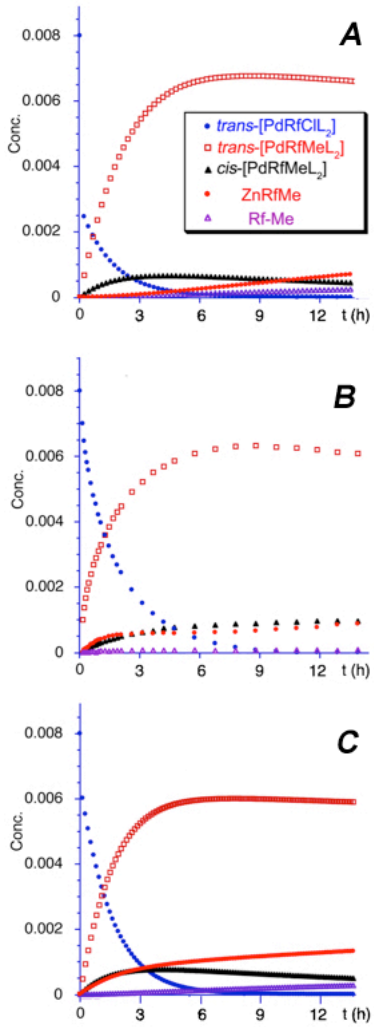

Figure 4. Experimental plot (**B**) for the transmetalation reaction of [PdRfCl(L)$_2$] **1** with $ZnMe_2$, and kinetic simulations following model I (**A**), or model II (**C**). The plots are shown as concentration versus time, using as starting concentrations: [**1**] = $8 \cdot 10^{-3}$M, [$ZnMe_2$] = $8 \cdot 10^{-2}$M, [PPh_3] = $4 \cdot 10^{-3}$M.

Considering the same set of equations of *model I*, but adding the formation of ZnRfMe by secondary transmetalation with Rf/Me exchange from complex **1,** through a ligand-dependent pathway sharing the trans-[PdClRf($ZnMe_2$)(PPh_3)] intermediate in *model I*, the overall picture (*Model II*) reproduces very well the formation of ZnRfMe. Thus, the early

intuition of van Asselt and Elsevier,[9] about the origin of homo biaryls in the reaction of in the reaction of [PdBzBr(ArBIAN)] (Bz = benzyl; Ar-BIAN = bis(arylimino)acenaphthene) with ZnTolCl, finds full support here for the cross coupling processes of sp^2-sp^3 carbons in which the direct reaction of $ZnMe_2$ and *trans*-[PdRfCl(PPh_3)$_2$] is confirmed as the dominant transmetalation mechanism when the concentration of *trans*-[PdRfCl(PPh_3)$_2$] is high.

Model II was used for the least squares fitting of the set of experimental data of reactions carried out with different concentrations of PPh_3, affording the kinetic rate constants for the transmetalation processes. The reaction profile and the experimental $\Delta G^{\ddagger}$ values from these fittings are shown in Figure 5.

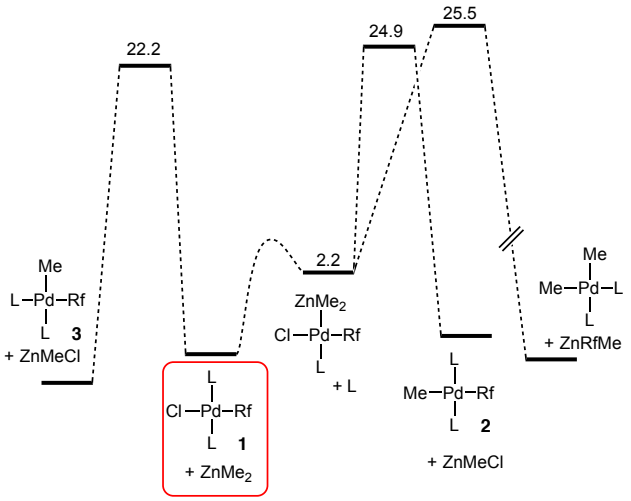

Figure 5. Experimental profile for the transmetalation pathways in the reaction between *trans*-[PdRfCl(PPh_3)$_2$] **1** and $ZnMe_2$. Free energies are in kcal/mol.

Obviously Figure 5 cannot reflect the effect of [PPh_3] on observed rates. Under low PPh_3 concentration, the equilibrium leading to formation of intermediate [PdRfCl(PPh_3)($ZnMe_2$)] is shifted to the right, and the transmetalation to form **2** is the fastest process. However, under moderate PPh_3 concentration the transmetalation reactions to form **2** or **3** have almost the same rate.

Conclusions

This study shows that unwanted Ar/Me transmetalations leading to ZnArMe can take place on complexes *trans*-[PdArXL$_2$], and also in *cis* and *trans*-[PdArMeL$_2$]. The exchange is faster on *trans*-[PdArXL$_2$], than on [PdArMeL$_2$] complexes, but the activation energies for them, and also for the desired transmetalation (Cl/Me exchange) are not very dissimilar, so all the exchanges are accessible at room temperature. In these circumstances, the specific features of the alkyl, aryl or halide groups involved, and the ancillary ligands, can be decisive. The faster pathways for the undesired Ar/Me exchange involve ligand-dependent associative substitution of phosphine by $ZnMe_2$ on the square-planar complexes, but direct (ligand-"independent") exchange pathways are also accessible, at least in complexes *trans*-[PdArMeL$_2$].

In catalysis, the formation of ZnArR (R = alkyl) derivatives leads to homocoupling products and should be avoided. The addition of an excess of phosphine reduces its formation rate, but also the transmetalation reaction rate. On the other hand, if the reductive elimination is slow (as this usually happens when sp^3 carbons are involved) the aryl/alkyl exchange on the coupling intermediates [PdArRL$_2$] takes place at a non-negligible rate. Thus the use of ligands bearing some ability to induce faster reductive eliminations is highly desirable.

Experimental section

General Methods. All reactions were carried out under N_2 or Ar in THF dried using a Solvent Purification System (SPS). NMR spectra were recorded on Bruker ARX 300, AV 400 or AV 500 instruments equipped with variable-temperature probes. Chemical shifts are reported in ppm from tetramethylsilane (^{1}H), and CCl_3F (^{19}F), with positive shifts downfield, at ambient probe temperature unless otherwise stated. The temperature for the NMR probe was calibrated with an ethylene glycol standard (high temperature) and with a methanol standard (low temperature).[29] In the ^{19}F and ^{31}P NMR spectra registered in non-deuterated solvents, a coaxial tube containing acetone-d_6 was used to maintain the lock ^{2}H signal, and the chemical shifts are reported from the CCl_3F signal in deuterated acetone. The compounds *trans*-[PdRfMe(PPh_3)$_2$] (**2**) and *cis*-[PdRfMe(PPh_3)$_2$] (**3**) were prepared as reported in the literature.[10]

Kinetic experiments. In a standard experiment a solution of palladium complex *trans*-[PdRfCl(PPh_3)$_2$] (**1**), *trans*-[PdRfMe(PPh_3)$_2$] (**2**) or *cis*-[PdRfMe(PPh_3)$_2$] (**3**) (10 mg, 1.13x10^{-2} mmol) and PPh_3 (0 to 6 mg; 0 to 2.3 x10^{-2} mmol) in THF (0.40 ml) was prepared in a RMN tube and cooled to -96 ºC. A solution of $ZnMe_2$ 2M in toluene (0.20 ml, 0.40 mmol) was added plus cold THF to make 0.60 ml of final volume. Then a coaxial capillary containing acetone-d_6 was added, and the sample was placed into the NMR probe thermostated at 25 °C. The kinetic experiments were followed by ^{31}P NMR or ^{19}F NMR and concentration-time data were acquired by integration of the NMR signals.

The kinetic models were fit to the measured concentration vs. time by nonlinear least-squares (NLLS) regression using the program COPASI.[30] The experimental data were arranged into the matrix, where the columns collect the time-dependent concentration profile of a particular species detected by 19F NMR. The proposed kinetic model was entered into the software program, as well as the known values for the constants measured independently, as specified below. The program produces a list of parameters (rate constants) and constructs a system of simultaneous ordinary differential equations that describe the change in concentration of each species with time. The rates constants were refined by NLLS regression until a best fit was found. The uncertainties of the fitted constants correspond to the standard deviation of the least squares fitting, given by COPASI. To calculate the kinetic constants from the obtained concentration versus time data, the initial rate method was used. Only the first points (10% of the data) were taken into account to avoid the formation of Pd^0 species that alter the reaction rate

ASSOCIATED CONTENT

Electronic Supplementary Information (ESI) Available: Text, figures, tables, containing experimental and kinetic details and computational information.

AUTHOR INFORMATION

Corresponding Author

E-mail: espinet@qi.uva.es

E-mail: casares@qi.uva.es

E-mail: rar@uvigo.es

Notes

The authors declare no competing financial interests.

ACKNOWLEDGMENT

Financial support is gratefully acknowledged from the Junta de Castilla y León (Projects GR169 and VA256U13), and the Spanish MINECO (CTQ2013-48406-P, CTQ2012-37734 and CTQ2015-68794-P). We also thank Centro de Supercomputación de Galicia (CESGA, ICTS240-2013 and ICTS257-2014) for generous allocation of computing resources. J. del Pozo thanks Ministerio de Educación, Cultura y Deporte for FPU grant.

REFERENCES

1 a) Negishi E. *Angew. Chem. Int. Ed.* **2011**, *50*, 6738 – 6764 (Nobel lecture). (b) Handbook of Organopalladium Chemistry for Organic Synthesis; Ed. by Negishi, E. Wiley-Interscience: New York, 2002; Volume 1, Part III; (c) E. Negishi, X. Zeng, Z. Tan, M. Qian, Q. Hu, Z. Huang, Chapter 15 in "Metal-Catalyzed Cross-Coupling Reactions". Ed. by A. de Meijere, F. Diederich, Wiley-VCH. 2004.

2 For recent reviews of Negishi reaction see: (a) R. Jana, T. P. Pathak and M. S. Sigman, *Chem. Rev.*, **2011**, *111*, 1417–1492. (b) X.-F. Wu, P. Anbarasan, H. Neumann and M. Beller, *Angew. Chem., Int. Ed.*, **2010**, *49*, 9047–9050. Valente,C.; Belowich, M. E.; Hadei, N.; Organ, M. G. *Eur. J. Org. Chem.* **2010**, *23*, 4343–4354. (c) Phapale V. B.; Cardenas D. *J. Chem. Soc. Rev.* **2009**, *38*, 1598-1607. (d) Wuertz S.; Glorius F. *Acc. Chem. Res.* **2008**, 41, 1523-1533. (e) Fu, G. C. *Acc. Chem. Res.* **2008**, *41*, 1555-1564. (f) L. Jin, A. Lei. *Org. Biomol. Chem.*, **2012**, 10, 6817. (g) Valente, C.; Çalimsiz, S.; Hoi, K. H.; Mallik, D.; Sayah, M.; Organ, M. G. *Angew. Chem. Int. Ed.* **2012**, *51*, 3314–3332.

3 Recent examples of the Negishi reaction involving the cross-coupling of sp^3 carbon atoms: (a) Berretta G, Coxon G. D. *Tetrahedron Lett.* **2012**, *53*, 214–216. (b) Duez, S. Steib, A. K.; Paul Knochel, P. *Org. Lett.* **2012**, *14*, 1951-1953. (c) Duplais, C.; Krasovskiy, A.; Lipshutz, B. H.; *Organometallics* **2011**, *30*, 6090–6097. (d) Tanaka, M.; Hikawa, H.; Yokoyama, Y. *Tetrahedron*, **2011**, 67, 5897-5901. (e) Hunter, H. N.; Hadei, N.; Blagojevic, V.; Patschinski, P.; Achonduh, G. T.; Avola, S.; Bohme, D. K.; Organ M. G. *Chem. Eur. J.* **2011**, *17*, 7845–7851. (f) Krasovskiy, A.; Thomé, I.; Graff, J.; Krasovskaya, V.; Konopelski, P.; Duplais, C.; Lipshutz, B. H. *Tetrahedron Lett.* **2011**, *52*, 2203–2205. (g) Zhang, Ting; Gao, Xiaodi; Wood, Harold B. Tetrahedron Lett. **2011**, *52*, 311–313. (h) Hadei, N.; Achonduh, G. T.; Valente, C.; Brien, C. J. O.; Organ, M. G. *Angew. Chem. Int.* Ed. 2011, *50*, 3896–3899. (i) Nishihara, Y.; Okada, Y.; Jiao, J.; Suetsugu, M.; Lan, M.-T.; Kinoshita, M.; Iwasaki, M.; Takagi K. *Angew. Chem. Int. Ed.* 2011, *50*, 8660 –8664. (j) Calimsiz, S.; Organ, M. G. *Chem. Commun.* **2011**, *47*, 1598-1600. (k) Bernhardt, S.; Manolikakes, G.; Kunz, T.; Knochel, P. *Angew. Chem. Int. Ed.* **2011**, *50*, 9205 –9209.

4 Reviews covering the cross-coupling of sp3 carbon: (a) Li, H.; Seechurn, C. C. C. J.; Colacot T. *J. ACS Catal* **2012**, *2*, 1147–1164. (b) Netherton, M. R.; Fu, G. C. *Adv. Synth. Catal.* **2004**, 346, 1525-1532. (c) Frisch, A. C.; Beller, M. *Angew. Chem., Int. Ed.* **2005**, *44*, 674-688.

5 (a) McCann, L. C.; Hunter, H. N.; Clyburne, J. A. C.; Organ, M. G. *Angew. Chem. Int. Ed.* **2012**, *51*, 7024-7027. (b) McCann, L. C.; Organ, M. G. *Angew. Chem. Int. Ed.* **2014**, *53*, 4386-4389, and references therein.

6 a) García-Melchor, M.; Fuentes, B.; Casares, J. A.; Ujaque, G.; Lledós, A.; Maseras, F.; Espinet, P. *J. Am. Chem. Soc.* **2011**, *133*, 13519-13526. (b) Fuentes B.; Garcia-Melchor, M.; Lledós, A.; Maseras, F.; Casares, J. A.; Ujaque, G.; Espinet. P. Chem. Eur. J., 2010, 16, 8596-8599.

7 (a) Thaler, T.; Haag, B.; Gavryushin, A.; Schober, K.; Hartmann, E.; Gschwind, R. M.; Zipse, H.; Mayer, P.; Knochel, P. *Nat. Chem.* **2010**, *2*, 125-130. (b) Haas, D.; Hammann, J. M.; Greiner, R.; Knochel, P. *ACS Catal.*, **2016**, *6*, 1540–1552.

8 See for instance: Gioria, E.; Martínez-Ilarduya, J. M.; Espinet, P. *Organometallics*, **2014**, *33*, 4394–4400.

9 van Asselt, R.; Elsevier, C. J. *Organometallics*, **1994**, *13*, 1972–1980.

10.- Casares, J. A.; Espinet, P.; Fuentes, B.; Salas, G. *J. Am. Chem. Soc.*, **2007,** 129, 3508-3509.

11 For recent studies on the transmetalation of aryl and allylzinc see: (a) Liu, Q.; Lan, Y.; Liu, J.; Li, G.; Wu, Y. D.; Lei, A. *J. Am. Chem. Soc.*, **2009**, *131,* 10201–10210. (b) Li, J.; Jin, L.; Liu, C.; Lei, A. *Chem, Commun.* **2013**, *49*, 9615-9617. (c) Li, J.; Jin, L.; Liu, C.; Lei, A. *Org. Chem. Front.* **2014**, *1*, 50-53. (d) Yang, Y.; Mustard, T. J. L.; Cheong, P. H.-Y.; Buchwald, S. L. *Angew. Chem. Int. Ed.* **2013**, *52,* 14098-14102.

12 These are reactions in which an organopalladium complex acts as arylating or alkylating reagent towards another metal halide, such ZnRX. The reaction has been also reported and studied for the Stille Cross-Coupling: Pérez-Temprano, M. H.; Nova, A.; Casares, J. A.; Espinet, P. *J. Am. Chem. Soc.* **2008**, *130*,10518-10519.

13 Pérez-Rodríguez, M.; Braga, A.A. C.; García-Melchor, M.; Pérez-Temprano, M. H.; Casares, J.A.; Ujaque, G.; de Lera, A.R.; Álvarez, R.; Maseras, F.; Espinet, P. *J. Am. Chem. Soc.* **2009**, *131*, 3650-3657, and references therein

14 Note, for instance, that Ar–Ar coupling of perhalogenated aryls, has such a high activation energy, that it allows for the existence of many very stable cis-[PdAr2L2] complexes: (a) Usón, R.; Fornies, *J. Adv. Organomet. Chem.* **1988**, 28, 219-297. (b) Alonso, M.A.; Casares, J. A.; Espinet, P.; Martinez-Ilarduya, J. M.; Perez-Briso, C. *Eur. J. Inorg. Chem.* **1998**, *11*, 1745-1753. (c) Espinet, P.; Martínez-Ilarduya, J. M.; Perez-Briso, C.; Casado, A.L. ; Alonso, M.A. *J. Organomet. Chem.* **1998**, *551* (1-2), 9-20. (d) Bartolomé, C.; Espinet, P.; Villafañe, F.; Giesa, S.; Martin, A.; Orpen, A. G. *Organometallics* **1996**, *15*, 2019-2028

15 delPozo, J.; Gioria, E.; Casares, J.A.; Álvarez, R.; Espinet, P. *Organometallics*, **2015**, *34*, 3120–3128.

16 The details of both approaches (kinetic evolutions, and mathematical work up for the experimental studies; structural data for the calculations) are too long and are given as SI.

17 Except with alternative approaches, for instance when the reverse reaction can be studied. See an example in ref. 12.

18 The oxidative addition of RfI to $Pd(PPh_3)_4$ produces initially cis-$[PdRfI(PPh_3)_2]$, which then isomerizes to the trans isomer. See: Casado, A. L.; Espinet, P. *Organometallics* **1998**, 17, 954-959.

19 For short we do not specify at this time the Pd isomer involved, so we use a general representation for cis and trans. Note, however, that isomerization can occur during transmetalation. Note also that these transmetalations are highly reversible, regardless of the displacement of the equilibrium to one side or the other.

20 Note, however, that the amount of **3** formed during the reaction is so small that this result does not affect the overall behavior of the disappearance of **1**.

21 The rate of the reactions (whether with or without added PPh_3) is also very sensitive to the presence of Pd(0) (presumably $Pd(PPh_3)_2$), which is eager to coordinate more PPh_3 to produce $[Pd(PPh_3)_3]$. The consequence is that, since reductive elimination is retarded by free PPh_3, the formation of palladium(0) by reductive elimination has an autocatalytic effect on the reductive elimination. This effect would mislead the interpretation of the reaction rates measured in the absence of added PPh_3.

[22]Althought the kinetic experiments have been developed with $C_6Cl_2F_3$ (Rf) (which provides simple NMR spectra with more reliable integrations) and PPh_3. The DFT study was developed with a simpler models (Ar = C_6F_5 (Pf) and PPh_3 as ligand). We have shown that there is no significant difference in activation energies for C_6F_5 instead of $C_6Cl_2F_3$.

[23] Frisch, M. J.; Trucks, G. W.; Schlegel, H. B.; Scuseria, G. E.; Robb, M. A.; Cheeseman, J. R.; Scalmani, G.; Barone, V.; Mennucci, B.; Petersson, G. A.; Nakatsuji, H.; Caricato, M.; Li, X.; Hratchian, H. P.; Izmaylov, A. F.; Bloino, J.; Zheng, G.; Sonnenberg, J. L.; Hada, M.; Ehara, M.; Toyota, K.; Fukuda, R.; Hasegawa, J.; Ishida, M.; Nakajima, T.; Honda, Y.; Kitao, O.; Nakai, H.; Vreven, T.; Montgomery, J. A.; Peralta, J. E.; Ogliaro, F.; Bearpark, M.; Heyd, J. J.; Brothers, E.; Kudin, K. N.; Staroverov, V. N.; Kobayashi, R.; Normand, J.; Raghavachari, K.; Rendell, A.; Burant, J. C.; Iyengar, S. S.; Tomasi, J.; Cossi, M.; Rega, N.; Millam, J. M.; Klene, M.; Knox, J. E.; Cross, J. B.; Bakken, V.; Adamo, C.; Jaramillo, J.; Gomperts, R.; Stratmann, R. E.; Yazyev, O.; Austin, A. J.; Cammi, R.; Pomelli, C.; Ochterski, J. W.; Martin, R. L.; Morokuma, K.; Zakrzewski, V. G.; Voth, G. A.; Salvador, P.; Dannenberg, J. J.; Dapprich, S.; Daniels, A. D.; Farkas; Foresman, J. B.; Ortiz, J. V.; Cioslowski, J.; Fox, D. J., Gaussian 09, Revision B.01, Wallingford CT, 2009.

[24] See supporting information for data regarding PMe_3

25 A maximum rate limit without ligand substitution was estimated assuming that this were the only pathway under the maximum concentration of PPh_3 used. Conversely, assuming this maximum value, a minimum value for the rate of the pathway involving the ligand substitution was obtained (see SI).

[26] The palladium and zinc interaction does not have kinetic relevance. We have previously characterized computationally this kind of bimetallic complexes: (a) Álvarez, R.; de Lera, A. R.; Aurrecoechea, J. M.; Durana, A. *Organometallics* **2007**, *26*, 2799-2802. (b) González-Pérez, A. B.; Álvarez, R.; Faza, O. N.; de Lera, A. R.; Aurrecoechea, J. M. *Organometallics*, **2012**, *31*, 2053- 2058. (c) Lorenzo, P.; Aurrecoechea, J. M.; de Lera, A. R.; Álvarez, R. Eur. J. Org. Chem. **2013**, *13*, 2621-2626. (d) Arrate, M.; Durana, A.; Lorenzo, P.; de Lera, A. R.; Álvarez, R.; Aurrecoechea, J. M. *Chem. A Eur. J.* **2013** *19*, 13893–13900.

27 The kinetic scheme does not presume any interaction between Zn and chlorine or any other atom in the intermediate formed by substitution of PPh_3 by $ZnMe_2$.

28 For the stronger σ-donor ligand $PMePh_2$ the direct (ligand-independent) substitution pathway seems to be dominant, see ref. 6

29 Amman, C.; Meier, P.; Merbach, A. E. *J. Magn. Reson.* **1982**, *46*, 319-321.

30 COmplex PAthway SImulator. Hoops, S.; Sahle, S.; Gauges, R.; Lee, C.; Pahle, J.; Simus, N.; Singhal, M.; Xu, L.; Mendes, P.; Kummer, U. *Bioinformatics* **2006**, *22*, 3067–3074.